Macromolecules **1996,** *29,* 8487−8491

Wetting Behavior of Polymer Melts on Polydisperse Grafted Polymer Layers

Kenneth R. Shull

Department of Materials Science and Engineering, Northwestern University, Evanston, Illinois 60208-3108

Received June 3, 1996; Revised Manuscript Received September 23, 1996⊗

ABSTRACT: The thickness dependence of the free energy of a polymeric film is calculated for monodisperse melts on grafted polymer layers of the same composition. For monodisperse grafted layers, a comparison is made between the full equilibrium (constant chemical potential) case and the restricted equilibrium (constant grafting density) case. Results for the two situations are nearly identical, indicating that previous results obtained for full equilibrium conditions are valid for restricted equilibrium conditions as well. A monodisperse polymer on a polydisperse grafted layer, consisting of loops and tails of different lengths, is also considered. A simple statistical analysis indicates that a layer produced by uniform adsorption of all segments of the polymer chain will be dominated by relatively long tails. Calculations for representative loop and tail distributions give a monotonically decreasing free energy with increasing film thickness. The absence of an attractive minimum at a finite film thickness means that thin films of all thicknesses are stable, with no thermodynamic driving force for dewetting. The situation changes if both ends of the adsorbed molecules are grafted to the surface, giving an adsorbed layer consisting only of loops. In this case, the stabilizing influence of the tails is eliminated, and dewetting is predicted even for a polydisperse distribution of loops.

Introduction

For entropic reasons, the contact angle a polymer melt makes with a grafted polymer layer of identical composition is not necessarily zero.[1−4] This phenomenon is referred to as "wetting autophobicity", because the liquid in question (a polymer melt in this case) will not spread out over a thin, adsorbed layer of itself but will instead form individual droplets which make a finite contact angle with the adsorbed layer. The effect was observed long ago by Zisman for fatty acid derivatives.[5] For these relatively small molecules, the effect can be explained primarily in terms of dispersive interactions. The high surface energy head groups adsorb preferentially to the surface, leaving a layer of low surface energy "tails" with a thickness of several angstroms, from which the rest of the liquid will dewet. The physical origins of wetting autophobicity in polymeric systems are somewhat different and can be attributed to limitations on the molecular configurations of a polymer melt which is confined to a very thin layer. The thickness of an adsorbed polymer layer is similar to the radius of gyration, R_g, which is typically on the order of 100 Å. Dispersive interactions can often be neglected over these length scales, in which case the autophobic effect can be attributed to the configurational entropy of the polymer molecules. Wetting autophobicity can have important consequences in technological applications involving thin polymer films. Lubricant layers on magnetic recording media, for example, consist of perfluoropolyethers which interact with a surface via one or both ends of the polymer molecules. Many of these films are found to break up into droplets when the film thickness exceeds a critical value,[6] a result which can significantly affect the performance of the recording device. Another consequence of wetting autophobicity is that individual particles will tend to segregate preferentially to the surface of a polymer melt to which they have been grafted, as shown schematically in Figure 1. For the nonwetting (autophobic) case there is an attractive interaction between the particle and a free surface. These attractive interactions, and the resultant surface segregation, have been observed for block copolymer micelles in high molecular weight polymer melts.[7] Attractive interactions between individual micelles appear for similar reasons; thus, the macroscopic phase behavior of block copolymer/homopolymer blends is governed by some of the same fundamental effects responsible for the wetting behavior of thin polymer films on grafted polymer matrices. In

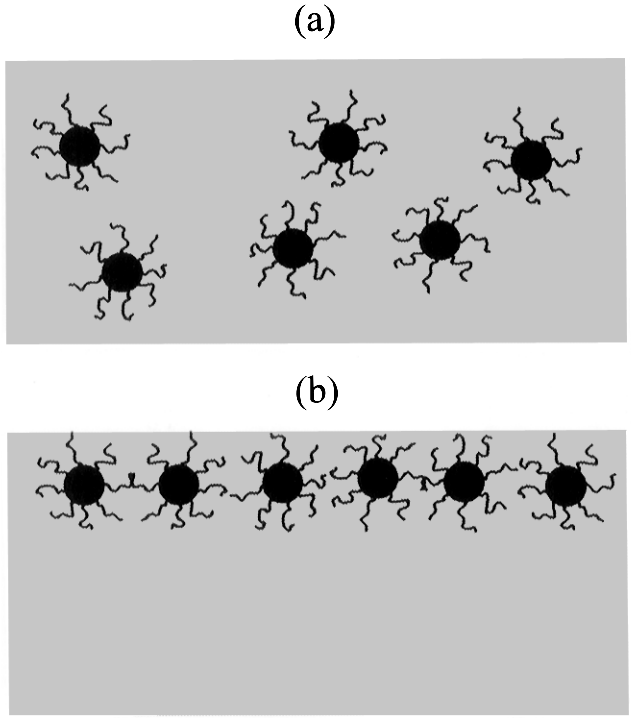

Figure 1. Surface segregation behavior for small particles with grafted polymers, dispersed in a homopolymer matrix with a composition identical to that of the grafted polymers. Particles exist preferentially at the free surface when the polymer melt does not wet the particles: (a) wetting case and (b) nonwetting (autophobic) case.

⊗ Abstract published in *Advance ACS Abstracts,* November 1, 1996.

S0024-9297(96)00797-8 CCC: $12.00

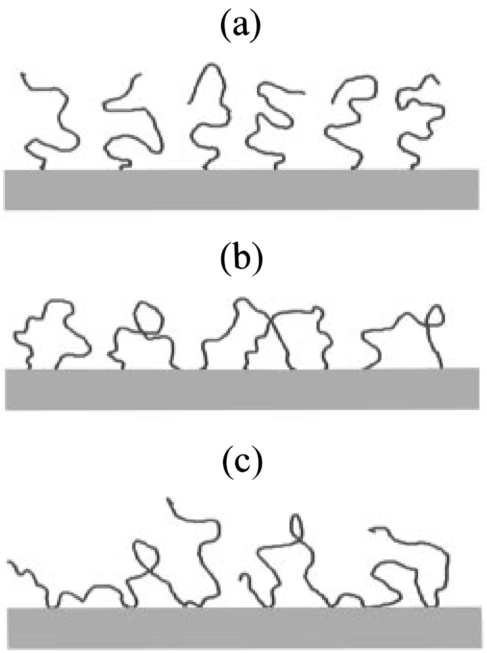

Figure 2. Schematic illustration of the different configurations of the adsorbed layer: (a) monodisperse tails resulting from grafting of one end of the polymer chains, (b) monodisperse loops resulting from grafting of both ends of the polymer chains, and (c) polydisperse mixture of loops and tails resulting from grafting of sites distributed throughout the polymer chains.

other words, a very high molecular weight homopolymer cannot be solubilized in an ordered domain morphology for the same reason that it cannot be spread, at equilibrium, as a thin film on top of a grafted polymer layer.

For the specific case of a grafted layer formed by end-attachment of monodisperse polymer chains, some analytic expressions for the contact angle have been derived by Leibler *et al.*[1] Because the factors involved can be quite complex, more accurate treatments of this problem require numerical approaches. Use of a numerical self-consistent mean-field theory enables one to calculate the free energy of the polymer film as a function of its thickness.[3,8] These calculations are based on an approximate enumeration of all possible chain configurations for a given thin-film geometry. For very thick films, the free energy of the film reaches a constant value characteristic of the bulk phase. Dewetting will occur if the free energy of the film is lower than this asymptotic value for some finite film thickness. The most important parameter with respect to the wetting properties is ΔF, the difference between this minimum free energy per unit area, and the free energy per unit area of a very thick film. For the small contact angles which are usually obtained in these situations, one has the following expression for the equilibrium contact angle, θ_e:[1,3]

$$\theta_{\mathrm{e}} = \sqrt{\frac{2\Delta F}{\gamma}} \tag{1}$$

where γ is the surface energy of the film.

In a previous publication, the wetting properties of two-component systems consisting of a homopolymer and an adsorbed polymer of identical chemical composition were considered.[3] The primary conclusion was that chains adsorbed in "loop" configurations (Figure 2b) contributed much more strongly to the dewetting than did chains adsorbed in "tail" configurations (Figure 2a). In both cases, finite contact angles were predicted whenever the molecular weight of the nonadsorbing species exceeded the molecular weight of the adsorbing species. Monodisperse loops and tails can be obtained experimentally with monolayers of diblock or triblock copolymers, but more generally applicable grafting schemes often involve grafting from sites distributed along the length of a polymer molecule. In these situations, the grafted layer is quite polydisperse, consisting of loops and tails of different molecular lengths (Figure 2c). All of these loops and tails have molecular weights which are less than the molecular weight of the polymer molecule from which they were formed. One then expects, on the basis of the results mentioned above for monodisperse loops and tails, that dewetting of the polymer might result. The primary goal of the work described here is to understand how the polydispersity of the grafted layer affects the wetting properties. The model system considered is a monodisperse polymer melt which is grafted to the surface through all possible segments along the polymer chain. The theoretical treatment is outlined in the next section, followed by a discussion of our results.

Theory

The numerical self-consistent-field treatment used here is identical to that which has been described in previous references.[3,9,10] Readers are referred to these references for a more complete description of the equations which are given here. The central quantities are distribution functions q_{k1} and q_{k2}, which describe the statistics of the two chain ends of a polymer with a degree of polymerization N_k. These expressions obey recursion relationships of the following form:

$$q_{k1}(i,j) = \left\{\frac{1}{6}q_{k1}(i-1,j-1) + \frac{1}{6}q_{k1}(i+1,j-1) + \frac{4}{6}\mathrm{q}_{k1}(i,j-1)\right\} \exp\left(-\frac{\mathrm{w}(i)}{k_{\mathrm{B}}T}\right) \tag{2}$$

where '*i*' indicates the the position and '*j*' indicates the specific repeat unit being considered. The quantity $\mathrm{w}(i)$ is a spatially dependent mean-field which depends on the local composition:

$$w(i) = \Pi(i)v - k_{\mathrm{B}}T\sum_{k}\frac{\phi_k(i)}{\mathrm{N}_k} \tag{3}$$

Here ϕ_k is the volume fraction of component k, v is the segmental volume, N_k is the degree of polymerization of component k, and Π is an osmotic pressure term which satisfies the incompressibility constraint.

The volume fraction corresponding to a particular polymeric component is given by the following summation:

$$\phi_k(i) = \frac{1}{N_k}\exp\left(\frac{\mu_k}{k_{\mathrm{B}}T} - 1\right)\sum_{j=1}^{N_k} q_{k1}(i,j)\ \mathrm{q}_{k2}(i,N_{k-j}) \tag{4}$$

where μ_k is the chemical potential of component k (defined as zero for the pure component). Equations 2−4 are solved self-consistently to give the volume fraction profiles for the different components in the system. For the constant coverage calculations, the chemical potentials are adjusted so that the integrated excesses remain constant as the thickness of the system (i.e., the number of lattice layers, L) changes. The free energy per unit area, F, for the fixed coverage case is obtained as follows:

$$F(e{=}La) = \frac{a}{v}\sum_{i=1}^{L}\left\{\sum_{k}\frac{\mu_k\phi_k(i)}{N_k} - \Pi(i)v\right\} \tag{5}$$

where L is the number of lattice layers and a is the statistical segment length. The free energy for the fixed chemical potential case is obtained from the osmotic pressure term:

$$F(e{=}La) = -a\sum_{i=1}^{L}\Pi(i) \tag{6}$$

The quantity $P(e)$ is defined as the difference between the actual free energy per unit area and the free energy per unit area for very thick films:

$$P(e) = F(e) - \mathrm{F}(\infty) \tag{7}$$

These expressions are used to generate the free energy curves discussed below. For generality, $P(e)$ is normalized by multiplying by $V/\mathrm{R}_g k_B T$, where V is the volume occupied by an adsorbed or grafted molecule, R_g is its unperturbed radius of gyration, k_B is Boltzmann's constant, and T is the absolute temperature.

Results and Discussion

Our first aim is to examine the difference between results obtained at fixed chemical potential (full equilibrium) and at fixed coverage (restricted equilibrium). It was pointed out previously that for the full equilibrium case, the adsorbed amount of brush chains does not necessarily remain constant as the thickness of the film is decreased.[3] There must, therefore, be some difference in free energy for the two cases as well. Qualitatively, it is clear that the free energy for the restricted equilibrium case must be at least slightly higher, because the restriction of fixed coverage represents an additional constraint on the system. The restricted equilibrium situation is more representative of the typical experimental situation where the brush chains are covalently attached to the surface of interest. Fortunately, enforcing a fixed grafting density of the grafted chains does not significantly alter the results, as can be seen from Figure 3. In this figure, we compare the thickness dependence of the free energy for monodisperse brushes adsorbed in loop configurations, for both the full equilibrium and restricted equilibrium situations. The free energy in the restricted equilibrium case is indeed slightly larger than the free energy for the fixed chemical potential case, but the difference is not at all significant. Our original conclusion that loops contribute more than tails to the dewetting tendency is still valid in this case. There is no guarantee, however, that the difference between restricted and full equilibrium will remain small when polydisperse brushes are considered. We consider only the restricted equilibrium case in the following discussion of polydisperse grafted brushes.

When addressing the issue of polydispersity within the grafted layer, one would like to study a distribution of loops and tails which is somehow representative of the actual situation. A useful reference distribution is the one that would be obtained by equilibrating a monodisperse polymer melt above a solid surface and instantaneously grafting all of the segments which are in direct contact with the surface. The structural features of the grafted layer can be calculated by the procedure described in the Appendix. The key quantities are $\phi_{\mathrm{loop}}(z,L)$ and $\phi_{\mathrm{tail}}(z,L)$, the respective polymer volume fractions arising from loops and tails of length L, at a distance z away from the grafting surface. The relative numbers of loops and tails of different lengths can be quantified by considering the following integrated volume fractions:

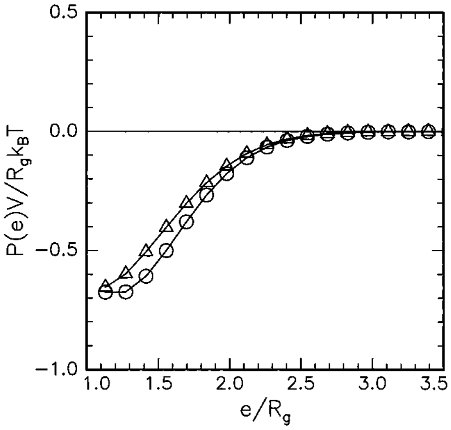

Figure 3. Normalized free energy per unit area as a function of film thickness for a polymer melt on a layer of chains grafted in loop configurations. The two curves are a comparison of the constant chemical potential (full equilibrium) data (○) with the data at constant coverage (restricted equilibrium) (Δ). Both curves have $z^*_{\mathrm{loop}}/R_g = 1$ for high film thicknesses, but the coverage changes by as much as 17% for the constant chemical potential data.

$$z^*_{\mathrm{loop}}(L) = \int_0^\infty \phi_{\mathrm{loop}}(z,L)\,\mathrm{d}z \tag{8}$$

$$z^*_{\mathrm{tail}}(L) = \int_0^\infty \phi_{\mathrm{tail}}(z,L)\,\mathrm{d}z \tag{9}$$

We can also sum over all possible values of L to obtain the overall volume fraction profiles for loops and tails:

$$\phi_{\mathrm{loop}}(z) = \sum_{L=3}^{N}\phi_{\mathrm{loop}}(z,L) \tag{10}$$

$$\phi_{\mathrm{tail}}(z) = \sum_{L=2}^{N}\phi_{\mathrm{tail}}(L,z) \tag{11}$$

where N is the degree of polymerization of the polymer melt from which the grafted layer was formed. Finally, we can obtain the total amount of adsorbed polymer residing in the loop and tail fractions from the following expressions:

$$z^*_{\mathrm{loop}} = \int_0^\infty \phi_{\mathrm{loop}}(z)\,\mathrm{d}z = \sum_{L=3}^{N} z^*_{\mathrm{loop}}(L) \tag{12}$$

$$z^*_{\mathrm{tail}} = \int_0^\infty \phi_{\mathrm{tail}}(z)\,\mathrm{d}z = \sum_{L=2}^{N} z^*_{\mathrm{tail}}(L) \tag{13}$$

The relevant features of the idealized grafted layer being considered here are summarized by Figures 4 and 5. Figure 4 shows the overall volume fraction profiles corresponding to loops and tails. The calculated values

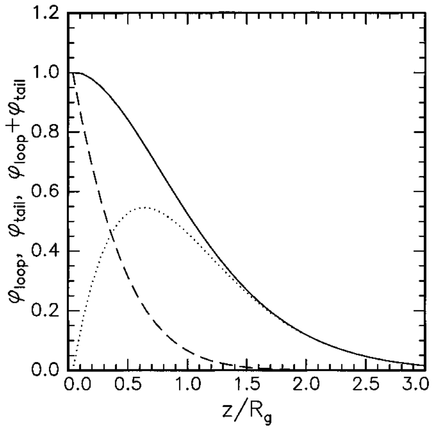

Figure 4. Volume fraction profiles of loops (- - -), tails (···), and combined loops and tails (—) for a polydisperse brush resulting from grafting all points of an equilibrated polymer that are initially in contact with the grafting surface.

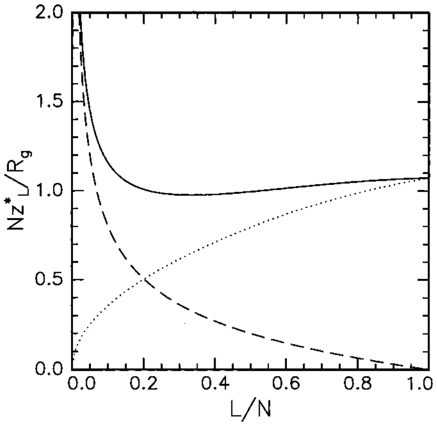

Figure 5. Integrated volume fractions of loops (- - -), tails (···), and combined loops and tails (—) for the polydisperse brush as a function of the normalized length of the loops or tails.

for $z^*_{\rm loop}$ and $z^*_{\rm tail}$ are $0.38R_g$ and $0.75R_g$, respectively, where R_g is the unperturbed radius of gyration of the monodisperse polymer from which the grafted layer was produced ($R_g = a(N/6)^{1/2}$). Note that the majority of the polymer in the grafted layer is in the form of tails. As one would expect, the outer portion of the grafted layer is dominated by tails, whereas the portion of the layer in the vicinity of the grafting surface is dominated by loops. The distribution of lengths among the loop and tail fractions is shown in Figure 5. In this figure, normalized values of $z^*_{\rm loop}(L)$ and $z^*_{\rm tail}$(L) are plotted as a function of L/N.

The idealized, polydisperse grafted layer considered here is dominated by long tails and short loops, with the total amount of polymer present in tails exceeding the total amount of polymer present in loops by a factor of 2. It seems reasonable to expect that these features will persist in general when the grafting sites are distributed uniformly along the polymer backbone. Our main conclusion with regard to the wetting behavior in these sorts of systems is that the polydispersity in lengths for the loops and tails can easily eliminate any tendency to give wetting autophobicity. This result is illustrated in Figure 6. Part a of this figure shows a discretized distribution of loops and tails which is roughly consistent with the continuous distributions from Figure 5. Part b of Figure 6 shows the calculated free energy vs thickness for the film, for restricted equilibrium conditions. The free energy increases monotonically as the film thickness is decreased. The absence of a minimum in the free energy at a finite film thickness indicates that wetting autophobicity is not predicted for this system. This distribution is just one out of a large number that could be chosen to approximate the idealized continuous distribution shown in Figure 5, but other similar distributions show the same effect. Our conclusion from these calculations is that a thin polymer film, placed on a surface with which it reacts to form covalent bonds, is likely to be thermodynamically stable, with no tendency to dewet. The wetting behavior here is dominated by the large numbers of relatively long tails that are expected to exist. This situation changes when the ends of the molecules are grafted to the surface. Wetting autophobicity is predicted in these cases, for all distributions of loop sizes that have been examined.

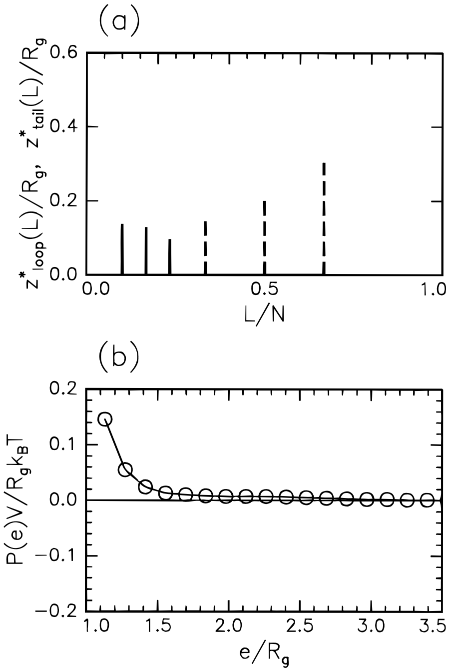

Figure 6. (a) Bar graph showing the distribution of loops (solid lines) and tails (dashed lines) in a model adsorbed layer. (b) Free energy as a function of film thickness for the distribution of loops and tails from part a. Fixed coverage (restricted equilibrium) conditions were assumed.

Summary

Previous results have shown that the thermodynamic tendency of a monodisperse polymer to dewet a grafted layer of the same composition is greater when the chains are grafted in loop configurations than when chains are grafted in tail configurations. This result, obtained from full equilibrium calculations where the chemical potential of the grafted chains is constant, remains valid for the more realistic restricted equilibrium situation, where the number of chains in the grafted layer is fixed. In addition, the predicted contact angles for the full equilibrium and restricted equilibrium cases are nearly identical. Adsorbed layers consisting of a distribution of loops and tails of different lengths are less likely to produce a driving force for dewetting. Adsorbed layers formed by the uniform grafting of all segments along the backbone of a polymer chain are dominated by relatively long tails, and these tails suppress the dewetting tendency associated with the loops. Wetting autophobicity is still predicted, however, when both ends of the molecules in the grafted layer are attached to the surface.

Acknowledgment. Support from the National Science Foundation (DMR-9457923) is gratefully acknowledged. Acknowledgment is also made to the Donors of The Petroleum Research Fund, administered by the American Chemical Society, for partial support of this research. The idea that the polydispersity of the grafted layer might significantly affect the wetting properties originates from a conversation with Dr. L. Leger.

Appendix: Distribution of Loops and Tails for an Equilibrated Polymer Melt.

The relative numbers of loops and tails of different lengths can be obtained from the distribution functions, as described in the book by Fleer *et al.*[10] In our case we can make several significant simplifying assumptions. Because the mean-field for a homogeneous polymer melt deviates significantly from zero only in the first lattice layer, we can use simple random walk statistics to obtain the numbers of loops and tails. Also, all repeat units of the polymer backbone are present at the interface at nearly equal concentrations. The number of tails is given by the number of random walks that originate from the surface, but never return to this surface. Similarly, the number of loops is determined by the number of random walks that originate and end at the surface, but otherwise never come in contact with the surface. The problem can be solved numerically by using the following recursion relationships for the distribution functions:

$$q_1(i,j) = \left\{\frac{1}{6}q_1(i-1,j-1) + \frac{1}{6}q_1(i+1,j-1) + \frac{4}{6}q_1(i,j-1)\right\} \tag{14}$$

$$q_2(i,j) = \left\{\frac{1}{6}q_2(i-1,j-1) + \frac{1}{6}q_2(i+1,j-1) + \frac{4}{6}q_2(i,j-1)\right\} \tag{15}$$

Here q_1 represents the end of a loop or tail originating from the surface, and q_2 represents the end of a tail which originates away from the surface. The initial conditions for q_1 and q_2 are determined from the requirement that these ends be at the surface ($i = 1$) or away from the surface ($i > 1$):

$$q_1(1,0) = 1, \quad q_1(i>1,0) = 0, \quad q_2(1,0) = 0, \quad q_2(i>1,0) = 1 \tag{16}$$

The boundary condition is determined by the requirement that the random walk does not return to the surface:

$$q_1(1,j>0) = q_2(1,j>0) = 0 \tag{17}$$

The first step in obtaining a solution for the distribution of loops and tails is to solve eqs 14 and 15 for all values of j from 1 to N, where N is the degree of polymerization of the polymer, and for a sufficiently large number of lattice layers, M, so that $q_1(M,N)$ is very small. The volume fraction corresponding to loops of length L is obtained from these distribution functions, keeping in mind that there are many possible loops of a given length. The maximum loop length is N, corresponding to the case where the two ends of the molecule are the only segments in contact with the surface. There are two possible loops with a length of $N - 1$, three possible loops with a length of $N - 2$, etc. In general, there are $N - L + 1$ possible loops with a length L. Similarly, there are two tails of length L that are possible, one for each end of the molecule. When these degeneracies are accounted for, the volume fractions, $\phi_{\text{loop}}(i,L)$ and $\phi_{\text{tail}}(i,L)$, corresponding respectively to loops and tails of length L, are given by the following expressions:

$$\phi_{\text{loop}}(i,L) = \frac{N - L + 1}{N}\sum_{j=1}^{N} q_1(i,j)\, q_1(i,L-j) \tag{18}$$

$$\phi_{\text{tail}}(i,L) = \frac{2}{N}\sum_{j=1}^{N} q_1(i,j)\, q_2(i,L-j) \tag{19}$$

References and Notes

(1) Leibler, L.; Ajdari, A.; Mourran, A.; Coulon, G.; Chatenay, D. In *Ordering in Macromolecular Systems;* Teramoto, A., Norisuje, M. K. T., Eds.; Springer-Verlag: Berlin, 1994; p 301.
(2) Liu, M.; Rafailovich, M. H.; Sokolov, J.; Achwarz, S. A.; Zhong, X.; Eisenberg, A.; Kramer, E. J.; Sauer, B. B.; Satija, S. *Phys. Rev. Lett.* **1994**, *73*, 440.
(3) Shull, K. R. *Faraday Discuss.* **1994**, *98*, 203.
(4) Reiter, G.; Schultz, J.; Auroy, P.; Auvray, L. *Europhys. Lett.* **1996**, *33*, 29.
(5) Hare, E. F.; Zisman, W. A. *J. Phys. Chem.* **1955**, *59*, 335.
(6) Min, B. G.; Choi, J. W.; Brown, H. R.; Yoon, D. Y.; O'Connor, T. M.; Jhon, M. S. *Tribol. Lett.* **1995**, *1*, 225.
(7) Shull, K. R.; Winey, K. I.; Thomas, E. L.; Kramer, E. J. *Macromolecules* **1991**, *24*, 2748.
(8) Shull, K. R. *J. Chem. Phys.* **1991**, *94*, 5723.
(9) Jones, R. A. L.; Norton, L. J.; Shull, K. R.; Kramer, E. J.; Felcher, G. P.; Karim, A.; Fetters, L. J. *Macromolecules* **1992**, *25*, 2359.
(10) Fleer, G. J.; Stuart, M. A. C.; Scheutjens, J. M. H. M.; Cosgrove, T.; Vincent, B. *Polymers at Interfaces*; Chapman and Hall: London, 1993.

MA9607978